SRTTU

JCARME
ISSN: 2228-7922
Journal of Computational and Applied Research in Mechanical Engineering
Vol. 10, No. 1, pp. 73-84
jcarme.sru.ac.ir

Dynamic response of a Pelton turbine shaft under the impact of water jet

Mahesh Chandra Luintel* **and Tri Ratna Bajracharya**

Department of Mechanical Engineering, Pulchowk Campus, Institute of Engineering, Tribhuvan University 44700, Nepal

Article info:
Type: Research
Received: 04/01/2019
Revised: 04/04/2019
Accepted: 14/04/2019
Online: 14/04/2019

Keywords:
Pelton turbine,
Flexible shaft,
Free response,
Forced response,
Impact of jet.

Abstract
The performance and reliability of any rotating machine can be studied by proper dynamic analysis of the machine. This paper presents a method to study the dynamic response of a Pelton turbine shaft due to the impact of a water jet. Equations of motion for the bending vibration of the Pelton turbine assembly, in two transverse directions, are developed using the Lagrange equation of motion with the help of assumed mode's method. The Pelton wheel is assumed as a rigid disk attached to an Euler-Bernoulli shaft. The impact provided by the water jet is represented in the form of a Fourier series. Critical speeds of the system are determined by performing free vibration analysis and presented in the form of the Campbell diagram. The response plots due to the impact of water are generated by performing forced response analysis. Both free and forced analyses are carried out by considering the first three modes of vibration.

1. Introduction

Most of the power-producing and power-consuming units consist of a disk attached to a shaft. One of the most common examples of such units is a Pelton turbine unit used for electricity generation in hydropower plants. Pelton turbines are high head turbines used for both small and large power generation. These rotating turbines are subjected to highly hostile working conditions. The design and manufacturing challenges are concerned with improvement in performance, life, and reduction in weight without loss of reliability. There are numerous possibilities of excitation by external disturbances and the behavior of the system under those disturbances can be predicted to some extent by the appropriate dynamic analysis.

The dynamic response of such a shaft-disk system depends upon many components and operating parameters. Different researchers investigated different aspects of a rotodynamic system by modelling the system as an assembly of a rigid disk attached to an Euler-Bernoulli shaft. Sabuncu et al. [1] investigated the critical speed of a rotor consisting of a single disc on a solid shaft by treating the shaft as a rotating beam element using a transfer matrix-finite element model. Rajalingham et al. [2] investigated the influence of external damping on rotor response to an imbalance of gravity excitations and showed that sufficient amount of

*Corresponding author
email address: mcluintel@ioe.edu.np

damping can suppress the reported instability caused by anisotropic bending stiffness characteristics. Lee et al. [3] analyzed the effect of the direction of application and magnitude of loads on the stability and natural frequency of flexible rotors subjected to non-conservative torque and force.

Khader et al. [4] investigated the stability of the rotating cantilever shaft with a rigid disk at its free end subjected to periodic follower axial force and end moment. Silva et al. [5] studied the bending vibration of a machine rotor using the Euler-Bernoulli beam theory, as a continuous beam, subjected to a specific set of boundary conditions. Chattoraj et al. [6] considered a two-dimensional isotropic and flexible horizontal rotor with symmetrical disk including the effects of gravity and Coriolis forces. Gundogdu et al. [7] presented simulations of a continuous cantilever beam and an unbalanced disk system by extending a classical Jeffcott rotor approach to a model that gives the first three (or more) modes of the flexible beam.

Shahgholi et al. [8] also investigated two-rotor systems, one of which was comprised of a symmetrical shaft and an asymmetrical disk, and the other one was comprised of an asymmetrical shaft and an asymmetrical disk. Lin et al. [9] used finite element simulation to develop several models of a single-rotor system, with different numbers of shaft elements, a relative number of degrees of freedom using four types of modelling for the shaft and disk interface. Han [10] performed complex harmonic analysis for rotor based upon Floquet theory and presented the modal features of each critical speed quantitatively and qualitatively. Huang [11] studied the characteristics of the torsional vibration of a rotor with unbalance by numerical simulation.

Some researchers studied non-linear phenomena in shaft-disk systems. Chang et al. [12] analyzed instability and non-linear dynamics of a simply supported slender shaft made of viscoelastic material and determined the stability. Genta et al. [13] extended the usual mathematical models based on the finite element method to the study of the dynamic behavior of rotors with non-constant angular speed by considering both the nonlinear behavior of the rotor and its geometrical or inertial anisotropy. Inoue et al. [14] investigated the chaotic vibration due to the 1 to (−1) type internal resonance at the major critical speed and twice the major critical speed. Diken et al. [15] considered a Jeffcott rotor and derived the non-linear dynamic equations of the rotor, and showed that there exists two subharmonic transient vibrations caused by the non-linearity of the system itself. Shad et al. [16] investigated the nonlinear dynamics of rotors by developing a mathematical model incorporating the higher-order deformations in bending, rotary inertia, gyroscopic effect, rotor mass unbalance, and dynamic axial force. Phadatare et al. [17] formulated strongly coupled non-linear equations of motion, based on strain energy and kinetic energy equations for shaft, disk, and unbalance mass, with shaft undergoing large bending deformations to determine the nonlinear frequencies and resultant dynamic behavior of the high-speed rotor-bearing system with mass unbalance. Similarly, some researchers investigated the coupled bending and torsional vibration of the shaft disk systems. Al-Bedoor [18] developed a model for coupled torsional and lateral vibrations of an unbalanced rotor and showed through simulation that there exists an energetic interaction between the rotor torsional and lateral vibration. Xiang et al. [19] studied the vibration characteristics on flexural and torsional modes of a Jeffcott rotor system with rigid support. Alnefaie et al. [20] considered a rotating flexible shaft-disk system to study the torsional vibration coupled with the lateral and longitudinal vibration, and showed that, while the shaft speed changes, the torsional natural frequency of the shaft-disk system and longitudinal natural frequency of the beam does not change but lateral natural frequency of the beam changes.

Another area dealt by many researchers is the dynamic response of the rotodynamic system due to a different kind of interactions on the disk of the system. Kojima et al. [21] investigated the torsional vibrations of a rotating shaft system having a disk and a magnet coupling in which the driver of the magnet coupling is excited by sinusoidal motion and the disk is subjected to the constant load torque.

Few research works have been carried out to study the effect of looseness on the behavior of the shaft-disk system. Muszynska et al. [22] presented the results of numerical simulation of the dynamic behavior of a one-lateral-mode rotor, which is unbalanced and radially side-loaded, with either a loose pedestal (looseness in a stationary joint) or with occasional rotor-to-stator rubbing in which the nonlinearities are associated with the rotor intermittent contacts with the stationary element. Behzad et al. [23] used the energy method to calculate rotor response with a loose rotating disk on it and showed that the clearance between the loose disk and shaft, shaft speed, mass and mass moment of inertia of disk have a major effect on a rotor response and beating phenomena.

Many researchers have extensively studied the effect of rub impact on the dynamic behavior of the shaft-disk system. Azeez et al. [24] worked to obtain the transient response of an overhung rotor undergoing vibro-impacts due to a defective bearing with reference to an overhung rotor clamped on one end, with a flywheel on the other and impacts occurring in between, due to a bearing with clearance. Shen et al. [25] investigated the vibration characteristics of a rub-impact rotor-bearing system excited by mass unbalance including mass eccentricity and initial permanent deflection. Jian et al. [26] studied the nonlinear dynamic analysis of the rotor-bearing system supported by oil-film short bearings, with nonlinear suspension, by considering the rub–impact between rotor and stator for precise analysis of rotor-bearing systems. Khanlo et al. [27] studied the chaotic vibration analysis of a rotating flexible continuous shaft-disk system with a rub impact. Khanlo et al. [28] also investigated the lateral-torsional coupling effects on the nonlinear dynamic behavior of a rotating flexible shaft–disk system. Jiao et al. [29] developed a dynamic model to study the characteristics of the unbalanced rotor system with external excitations including the influences of the gyroscopic effect, gravity and static/dynamic unbalance. Ma et al. [30] investigated the nonlinear dynamic characteristics of a single span rotor system with two discs under fixed-point and local arc rub-impact conditions. Tai et al. [31] investigated the stability and steady-state response of the rotor system using a lumped mass model of a single rub-impact rotor system considering the gyroscopic effect.

Wahab et al. [32] studied the parametric instability behaviou for a simple shaft and disk system subjected to axial load under pinned-pinned boundary condition and found that the additional disk mass decreases the instability region during thestatic condition and the location of the disk also has a significant effect on the instability region of the shaft. Chen et al. [33] developed a model based on the finite element method and Lagrange's equation to study the dynamic behavior of a flexible rotor system subjected to time-variable base motions and found that the base rotations would cause nonlinearities.

Most of the earlier papers have focused the dynamic response of a flexible shaft due to intervention from the surroundings such as rub impact or effects of bearing properties. This paper focuses mainly on the dynamic response of the shaft-disk system to the impact of general tangential forces on the disk which can be used to study the behavior of a Pelton turbine subjected to the impact of the water jet.

2. Problem formulation

2.1. System kinematics and energy expressions for the system

Fig. 1 shows a rigid disk attached to a flexible shaft. The axes *x*, *y*, and *z* are chosen such that *x* is along the longitudinal direction of the shaft, y is along the transverse direction of the shaft on the horizontal plane, and *z* is along the transverse direction of the shaft on the vertical plane. Similarly, transverse displacements of any point of the shaft along horizontal and vertical directions are $v(x,t)$ and $w(x,t)$, respectively. For the horizontal shaft, Pelton turbine water jet acts along the *y*-direction.

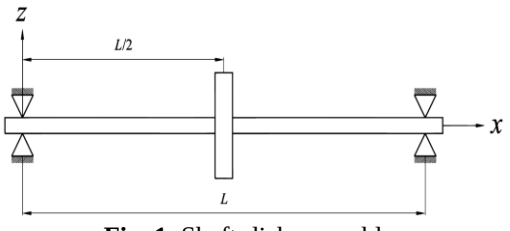

Fig. 1. Shaft-disk assembly.

The velocity of any point on the neutral axis of the shaft with reference to an inertial frame is given by [27]:

$$\boldsymbol{v_s} = (\dot{v} - \Omega w)\boldsymbol{j} + (\dot{w} + \Omega v)\boldsymbol{k} \quad (1)$$

The angular velocity vector of the shaft element is given by [27]:

$$\boldsymbol{\omega_e} = (\Omega + v'\dot{w}')\boldsymbol{i} + (-\Omega v' - \dot{w}')\boldsymbol{j} + (-\Omega w' + \dot{v}')\boldsymbol{k} \quad (2)$$

Then kinetic energy of the shaft is given by:

$$T = \frac{1}{2}\rho A \int_0^L [(\dot{v} - \Omega w)^2 + (\dot{w} + \Omega v)^2]dx + \frac{1}{2}\rho J_{ps} \int_0^L [(\Omega + v'\dot{w}')^2]\,dx + \frac{1}{2}\rho I_s \int_0^L [(-\Omega v' - \dot{w}')^2 + (-\Omega w' + \dot{v}')^2]\,dx \quad (3)$$

Avoiding higher-order terms, the kinetic energy of the shaft given by Eq. (3) can be expressed as:

$$\begin{aligned} T_s &= \frac{1}{2}\rho A \int_0^L \dot{v}^2 dx + \frac{1}{2}\rho A \int_0^L \dot{w}^2 dx \\ &+ \frac{1}{2}\rho A\Omega^2 \int_0^L v^2 dx + \frac{1}{2}\rho A\Omega^2 \int_0^L w^2 dx \\ &+ \rho A\Omega \int_0^L \dot{w} v dx - \rho A\Omega \int_0^L \dot{v} w dx + \frac{1}{2}\rho J_{ps}\Omega^2 L \\ &+ \rho J_{ps}\Omega \int_0^L \dot{w}' v'\,dx + \frac{1}{2}\rho I_s \int_0^L \dot{v}'^2 dx \\ &+ \frac{1}{2}\rho I_s \int_0^L \dot{w}'^2 dx + \frac{1}{2}\rho I_s\Omega^2 \int_0^L v'^2 dx \\ &+ \frac{1}{2}\rho I_s\Omega^2 \int_0^L w'^2 dx + \rho I_s\Omega \int_0^L \dot{w}' v'\,dx \\ &- \rho I_s\Omega \int_0^L \dot{v}' w'\,dx \end{aligned} \quad (4)$$

Similarly, the kinetic energy of the disk can be expressed as:

$$\begin{aligned} T_d &= \tfrac{1}{2}M_d(\dot{v}^2)\big|_{x=\frac{L}{2}} + \tfrac{1}{2}M_d(\dot{w}^2)\big|_{x=\frac{L}{2}} + \\ &\tfrac{1}{2}M_d\Omega^2(v^2)\big|_{x=\frac{L}{2}} + \tfrac{1}{2}M_d\Omega^2(w^2)\big|_{x=\frac{L}{2}} + \\ &M_d\Omega(\dot{w}v)\big|_{x=\frac{L}{2}} - M_d\Omega(\dot{v}w)\big|_{x=\frac{L}{2}} + \\ &\tfrac{1}{2}\rho_d h J_{pd}\Omega^2 + \rho_d h J_{pd}\Omega(\dot{w}'v')\big|_{x=\frac{L}{2}} + \\ &\tfrac{1}{2}\rho_d h I_d\left(\dot{v}'^2\right)\Big|_{x=\frac{L}{2}} + \tfrac{1}{2}\rho_d h I_d\left(\dot{w}'^2\right)\Big|_{x=\frac{L}{2}} + \\ &\tfrac{1}{2}\rho_d h I_d\Omega^2\left(v'^2\right)\big|_{x=\frac{L}{2}} + \\ &\tfrac{1}{2}\rho_d h I_d\Omega^2\left(w'^2\right)\big|_{x=\frac{L}{2}} + \\ &\rho_d h I_d\Omega(\dot{w}'v')\big|_{x=\frac{L}{2}} - \\ &\rho_d h I_d\Omega(\dot{v}'w')\big|_{x=\frac{L}{2}} \end{aligned} \quad (5)$$

The strain energy of the shaft due to the bending is then given by:

$$U_s = \frac{1}{2}EI_s \int_0^L [(v'')^2 + (w'')^2]dx \quad (6)$$

Work done by the impact of the jet is given by:

$$W_{ext} = F(t)(v)\big|_{x=\frac{L}{2}} \quad (7)$$

2.2. Equation of motion for the system

For the assumed mode method, displacement variables can be assumed as:

$$v = \{\phi(x)\}^T\{V(t)\} = \{\phi\}^T\{V\} \quad (8)$$

$$w = \{\phi(x)\}^T\{W(t)\} = \{\phi\}^T\{W\} \quad (9)$$

Substituting v and w into Eqs. (4 to 7) and using Lagrange equation:

$$\frac{d}{dt}\left(\frac{\partial T}{\partial \dot{q}}\right) - \frac{\partial T}{\partial q} + \frac{\partial U}{\partial q} - \frac{\partial W_{ext}}{\partial q} = 0 \quad (10)$$

The equations of motion for transverse vibrations are gotten as:

$$\rho A\int_0^L[\{\phi\}\{\phi\}^T\{\ddot{V}\}]dx + \rho I_s\int_0^L[\{\phi'\}\{\phi'\}^T\{\ddot{V}\}]dx + M_d[\{\phi\}_d\{\phi\}_d{}^T\{\ddot{V}\}] + \rho_d hI_d[\{\phi'\}_d\{\phi'\}_d{}^T\{\ddot{V}\}] - 2\rho A\Omega\int_0^L[\{\phi\}\{\phi\}^T\{\dot{W}\}]dx - 2\rho I_s\Omega\int_0^L[\{\phi'\}\{\phi'\}^T\{\dot{W}\}]dx - 2M_d\Omega[\{\phi\}_d\{\phi\}_d{}^T\{\dot{W}\}] - 2\rho_d hI_d\Omega[\{\phi'\}_d\{\phi'\}_d{}^T\{\dot{W}\}] - \rho J_{ps}\Omega\int_0^L[\{\phi'\}\{\phi'\}^T\{\dot{W}\}]dx - \rho_d hJ_{pd}\Omega[\{\phi'\}_d\{\phi'\}_d{}^T\{\dot{W}\}] - \rho A\Omega^2\int_0^L[\{\phi\}\{\phi\}^T\{V\}]dx - \rho I_s\Omega^2\int_0^L[\{\phi'\}\{\phi'\}^T\{V\}]dx - M_d\Omega^2[\{\phi\}_d\{\phi\}_d{}^T\{V\}] - \rho_d hI_d\Omega^2[\{\phi'\}_d\{\phi'\}_d{}^T\{V\}] + EI_s\int_0^L[\{\phi''\}\{\phi''\}^T\{V\}]dx - F(t)\{\phi\}_d = \{0\} \quad (11)$$

$$\rho A\int_0^L[\{\phi\}\{\phi\}^T\{\ddot{W}\}]dx + \rho I_s\int_0^L[\{\phi'\}\{\phi'\}^T\{\ddot{W}\}]dx + M_d[\{\phi\}_d\{\phi\}_d{}^T\{\ddot{W}\}] + \rho_d hI_d[\{\phi'\}_d\{\phi'\}_d{}^T\{\ddot{W}\}] + 2\rho A\Omega\int_0^L[\{\phi\}\{\phi\}^T\{\dot{V}\}]dx + \rho J_{ps}\Omega\int_0^L[\{\phi'\}\{\phi'\}^T\{\dot{V}\}]dx + 2\rho I_s\Omega\int_0^L[\{\phi'\}\{\phi'\}^T\{\dot{V}\}]dx + 2M_d\Omega[\{\phi\}_d\{\phi\}_d{}^T\{\dot{V}\}] + \rho_d hJ_{pd}\Omega[\{\phi'\}_d\{\phi'\}_d{}^T\{\dot{V}\}] + 2\rho_d hI_d\Omega[\{\phi'\}_d\{\phi'\}_d{}^T\{\dot{V}\}] - \rho A\Omega^2\int_0^L[\{\phi\}\{\phi\}^T\{W\}]dx - \rho I_s\Omega^2\int_0^L[\{\phi'\}\{\phi'\}^T\{W\}]dx - M_d\Omega^2[\{\phi\}_d\{\phi\}_d{}^T\{W\}] - \rho_d hI_d\Omega^2[\{\phi'\}_d\{\phi'\}_d{}^T\{W\}] + EI_s\int_0^L[\{\phi''\}\{\phi''\}^T\{W\}]dx = \{0\} \quad (12)$$

3. Response of the system

3.1. Discretization of equation of motion

For the assumed mode method, it can be assumed:

$$\phi_i = sin\left(\frac{i\pi x}{L}\right) \quad (13)$$

which is the eigenfunctions of a simply supported non-rotating beam.
Substituting $\{\phi\} = \{\phi_1 \quad \phi_2 \quad .... \quad \phi_n\}^T$ into Eqs. (11) and (12), a system of linear ordinary differential equations for each assumed mode can be obtained as:

$$M_i\ddot{V}_i(t) - C_i\dot{W}_i(t) + K_iV_i(t) = F_i(t) \quad (14)$$

$$M_i\ddot{W}_i(t) + C_i\dot{V}_i(t) + K_iW_i(t) = 0 \quad (15)$$

where

$$M_i = \frac{1}{2}\rho AL + \frac{\pi^2 i^2}{2L}\rho I_s + M_d\, sin^2\left(\frac{i\pi}{2}\right) + \frac{\pi^2 i^2}{L^2}\rho_d hI_d\, cos^2\left(\frac{i\pi}{2}\right) \quad (16)$$

$$C_i = \rho AL\Omega + \frac{\pi^2 i^2}{L}\rho I_s\Omega + \frac{\pi^2 i^2}{2L}\rho J_{ps}\Omega + 2M_d\Omega\, sin^2\left(\frac{i\pi}{2}\right) + \frac{2\pi^2 i^2}{L^2}\rho_d h I_d\Omega\, cos^2\left(\frac{i\pi}{2}\right) + \frac{\pi^2 i^2}{L^2}\rho_d h J_{pd}\Omega\, cos^2\left(\frac{i\pi}{2}\right) \quad (17)$$

$$K_i = \frac{2\pi^3 i^3}{4L^3}EI_s - \frac{1}{2}\rho AL\Omega^2 - \frac{1}{2L}\rho I_s\Omega^2 - M_d\Omega^2\, sin^2\left(\frac{i\pi}{2}\right) - \frac{\pi^2 i^2}{L^2}\rho_d h I_d\Omega^2\, cos^2\left(\frac{i\pi}{2}\right) \quad (18)$$

and

$$F_i = F(t)\, sin\left(\frac{i\pi}{2}\right) \quad (19)$$

3.2. Solution for free response of the system

For free vibration analysis, substituting $F(t) = 0$, Eqs. (14) and (15) reduce to:

$$M_i\ddot{V}_i(t) - C_i\dot{W}_i(t) + K_iV_i(t) = 0 \quad (20)$$

$$M_i\ddot{W}_i(t) + C_i\dot{V}_i(t) + K_iW_i(t) = 0 \quad (21)$$

Substituting:

$$V_i(t) = \bar{V}_i\, e^{\lambda_i t} \quad (22)$$

and

$$W_i(t) = \bar{W}_i\, e^{\lambda_i t} \quad (23)$$

into Eqs. (20) and (21), the characteristics equation of the system is obtained as:

$$M_i{\lambda_i}^4 + \left({C_i}^2 + 2K_iM_i\right){\lambda_i}^2 + {k_i}^2 = 0 \quad (24)$$

Eq. (24) is quadratic on ${\lambda_i}^2$ and its roots are given as:

$$({\lambda_i)_1}^2 = -\frac{1}{2}\left[\left\{\left(\frac{C_i}{M_i}\right)^2 + 2\frac{K_i}{M_i}\right\} - \sqrt{\left(\frac{C_i}{M_i}\right)^4 + 4\left(\frac{C_i}{M_i}\right)^2\frac{K_i}{M_i}}\right] \quad (25)$$

and

$$({\lambda_i)_2}^2 = -\frac{1}{2}\left[\left\{\left(\frac{C_i}{M_i}\right)^2 + 2\frac{K_i}{M_i}\right\} + \sqrt{\left(\frac{C_i}{M_i}\right)^4 + 4\left(\frac{C_i}{M_i}\right)^2\frac{K_i}{M_i}}\right] \quad (26)$$

Then, the natural frequencies corresponding to backward and forward whirls are respectively given by:

$$(\lambda_i)_1 = \sqrt{\frac{1}{2}\left[\left\{\left(\frac{C_i}{M_i}\right)^2 + 2\frac{K_i}{M_i}\right\} - \sqrt{\left(\frac{C_i}{M_i}\right)^4 + 4\left(\frac{C_i}{M_i}\right)^2\frac{K_i}{M_i}}\right]} \quad (27)$$

and

$$(\lambda_i)_2 = \sqrt{\frac{1}{2}\left[\left\{\left(\frac{C_i}{M_i}\right)^2 + 2\frac{K_i}{M_i}\right\} + \sqrt{\left(\frac{C_i}{M_i}\right)^4 + 4\left(\frac{C_i}{M_i}\right)^2\frac{K_i}{M_i}}\right]} \quad (28)$$

3.3. Determination of force due to water jet

During the one complete rotation of the Pelton wheel, the jet does not strike the buckets for certain intervals as there is a gap between two buckets. Hence, the force exerted by the water jet on the disk can be approximated by the series of pulses, as shown in Fig. 2, where $t_2 - t_1$ (= $t_4 - t_3$ = $t_6 - t_5$ = ..) is the duration of each pulse which is proportional to the bucket thickness to the circumference of the equivalent runner wheel, and T is the period of one revolution of the runner wheel.

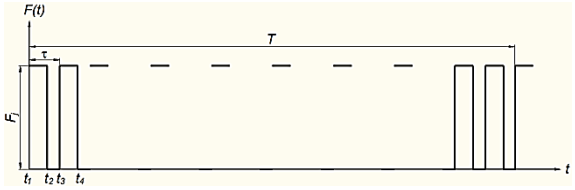

Fig. 2. Pulses of force due to the water jet on Pelton turbine.

The force due to the water jet can be defined for a period τ mathematically as:

$$F(t) = \begin{cases} F_j & t_1 \le t \le t_2 \\ 0 & t_2 < t < t_3 \end{cases} \quad (29)$$

Parameters required for calculation of the jet force F_j are taken from [34].
Since the force exerted by the water jet is periodic but non-harmonic, it is converted into harmonic terms using Fourier series expansion as:

$$F(t) = a_0 + \sum_{n=1}^{\infty} \left[a_n cos\left(\frac{2n\pi}{\tau} t\right) + b_n sin\left(\frac{2n\pi}{\tau} t\right) \right] \quad (30)$$

where

$$a_0 = \frac{1}{\tau} \int_0^{\tau} F(t) dt \quad (31)$$

$$a_n = \frac{2}{\tau} \int_0^{\tau} F(t)\, cos\left(\frac{2n\pi}{\tau} t\right) dt \quad (32)$$

and

$$b_n = \frac{2}{\tau} \int_0^{\tau} F(t)\, sin\left(\frac{2n\pi}{\tau} t\right) dt \quad (33)$$

3.4. Solution for forced response of the system

Using Eqs. (14) and (15) and Eq. (30), the forced vibration equation for i^{th} mode (where i is odd) of the system can be rewritten as:

$$M_i \ddot{V}_i(t) - C_i \dot{W}_i(t) + K_i V_i(t) = a_0 + \sum_{n=1}^{\infty} \left[a_n cos\left(\frac{2n\pi}{\tau} t\right) + b_n sin\left(\frac{2n\pi}{\tau} t\right) \right] \quad (34)$$

$$M_i \ddot{W}_i(t) + C_i \dot{V}_i(t) + K_i W_i(t) = 0 \quad (35)$$

Assuming steady-state response of i^{th} mode of the system due to n^{th} harmonics of force due to the water jet as:

$$[V_{ir}(t)]_n = \bar{V}_{0i} + (\bar{V}_{ci})_n\, cos\left(\frac{2n\pi}{\tau} t\right) + (\bar{V}_{si})_n\, sin\left(\frac{2n\pi}{\tau} t\right) \quad (36)$$

and

$$[W_{ir}(t)]_n = \bar{W}_{0i} + (\bar{W}_{ci})_n\, cos\left(\frac{2n\pi}{\tau} t\right) + (\bar{W}_{si})_n\, sin\left(\frac{2n\pi}{\tau} t\right) \quad (37)$$

Substituting Eqs. (36) and (37), into Eqs. (34 and 35), the expression for $(\bar{V}_{0i})_n$, $(\bar{V}_{ci})_n$, $(\bar{V}_{si})_n$, $(\bar{W}_{0i})_n$, $(\bar{W}_{ci})_n$ and $(\bar{W}_{si})_n$ are obtained which are required for the steady-state response of i^{th} mode of the system due to the n^{th} harmonics of force as:

$$\bar{V}_{0i} = \frac{a_0}{K_i} \quad (38)$$

$$(\bar{V}_{ci})_n = \frac{a_n(K_i\tau^2 - 4M_i\pi^2n^2)\tau^2}{16{M_i}^2\pi^4n^4 - 4\left({C_i}^2 + 2K_iM_i\right)\pi^2n^2\tau^2 + {K_i}^2\tau^4} \quad (39)$$

$$(\bar{V}_{si})_n = \frac{b_n(K_i\tau^2 - 4M_i\pi^2n^2)\tau^2}{16{M_i}^2\pi^4n^4 - 4\left({C_i}^2 + 2K_iM_i\right)\pi^2n^2\tau^2 + {K_i}^2\tau^4} \quad (40)$$

$$\bar{W}_{0i} = 0 \quad (41)$$

$$(\bar{W}_{ci})_n = -\frac{2b_nC_i\pi n\tau^3}{16{M_i}^2\pi^4n^4 - 4\left({C_i}^2 + 2K_iM_i\right)\pi^2n^2\tau^2 + {K_i}^2\tau^4} \quad (42)$$

and

$$(\bar{W}_{si})_n = \frac{2a_n C_i \pi n \tau^3}{16{M_i}^2\pi^4 n^4 - 4\left({C_i}^2 + 2K_i M_i\right)\pi^2 n^2 \tau^2 + {K_i}^2 \tau^4} \quad (43)$$

Then the steady-state response of i^{th} mode of the system due to all harmonics of force can be determined as:

$$V_{ir}(t) = \bar{V}_{0i} + \sum_{n=1}^{\infty}\left[(\bar{V}_{ci})_n \cos\left(\frac{2n\pi}{\tau}t\right) + (\bar{V}_{si})_n \sin\left(\frac{2n\pi}{\tau}t\right)\right] \quad (44)$$

and

$$W_{ir}(t) = \sum_{n=1}^{\infty}\left[(\bar{W}_{ci})_n \cos\left(\frac{2n\pi}{\tau}t\right) + (\bar{W}_{si})_n \sin\left(\frac{2n\pi}{\tau}t\right)\right] \quad (45)$$

Then the general forced response of the system due to all modes (i = 1, 2, 3,……m) is given by:

$$v_r(x\ t) = \sum_{i=1}^{m}\left[\left\{\bar{V}_{0i} + \sum_{n=1}^{\infty}\left[(\bar{V}_{ci})_n \cos\left(\frac{2n\pi}{\tau}t\right) + (\bar{V}_{si})_n \sin\left(\frac{2n\pi}{\tau}t\right)\right]\right\}\sin\left(\frac{i\pi x}{L}\right)\right] \quad (46)$$

Table 1. Parameters of the system.

Parameters	Value
Density of shaft material, ρ	7860 kg/m^3
Cross-sectional area of the shaft, A	0.8042×10^{-3} m^2
Length of the shaft, L	0.52 m
Modulus of elasticity of shaft material, E	202×10^9 GPa
Area moment of inertia of the shaft section, I_s	5.1472×10^{-8} m^4
Polar moment of area of the shaft section, J_{ps}	1.0294×10^{-7} m^4
Density of runner material, ρ_d	8550 kg/m^3
Mass of runner wheel, M_d	10.564 kg
Thickness of runner, h	35 mm
Area moment of inertia of the disk, I_d	0.5527×10^{-4} m^4
Polar moment of area of the shaft section, J_{pd}	0.11053×10^{-3} m^4

and

$$w_r(x\ t) = \sum_{i=1}^{m}\left[\left\{\sum_{n=1}^{\infty}\left[(\bar{W}_{ci})_n \cos\left(\frac{2n\pi}{\tau}t\right) + (\bar{W}_{si})_n \sin\left(\frac{2n\pi}{\tau}t\right)\right]\right\}\sin\left(\frac{i\pi x}{L}\right)\right] \quad (47)$$

4. Numerical results and discussion

To have an interpretation of the analytical expressions obtained for free and forced responses of the system, the values of system parameters are taken as listed in Table 1.

4.1 Critical speeds (natural frequencies) and Campbell diagram

Using Eqs. (16-18), equivalent mass (M_i), equivalent damping coefficient (C_i) and stiffness (K_i) for the first three modes are determined and shown in Table 2. Then, the natural frequencies corresponding to the backward and forward whirls can be found using Eqs. (27 and 28). This can be presented in the form of a Campbell diagram, as shown in Fig. 3. Natural frequencies of each mode corresponding to zero spin speed are the natural frequencies of the first three modes of the simply supported beam. As the spin speed increases, critical speed for the backward whirl of each mode decreases, whereas, the critical speed for a forward whirl for each mode increases. At lower speeds, bending stiffness will have a higher value than the stiffness due to the centrifugal effect (centrifugal stiffening). During backward whirl, centrifugal stiffening will act opposite to elastic restoring force and, therefore, critical speed for backward whirl decreases with the increase in spin speed, as shown in Fig. 3.

Table 2. Equivalent parameters for the first three modes.

Equivalent parameters	First mode	Second mode	Third mode
Mass (M_i)	12.2085 kg	4.0798 kg	12.2393 kg
Damping coefficient (C_i)	24.4247 Ω N.s/m	13.0384 Ω N.s/m	24.5478 Ω N.s/m
Stiffness (K_i)	(3.6223×10^6 – 12.2085 Ω^2) N.m	(5.7957×10^7 – 4.0798 Ω^2) N.m	(2.9341×10^8 – 12.2393 Ω^2) N.m

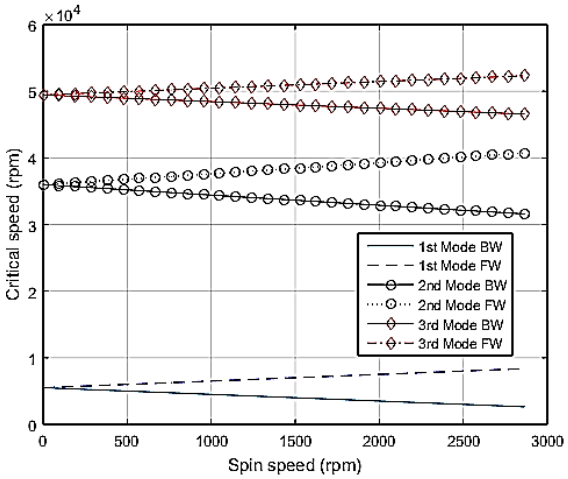

Fig. 3. Campbell diagrams for the first three modes.

During forward whirl, centrifugal stiffening will act in the same direction to elastic restoring force and, therefore, critical speed for forwarding whirl increases with the increase in spin speed, as shown in Fig. 3.

4.2. Fourier series representation of force due to the water jet

The values of variables F_j, t_2, and τ for the jet force shown in Fig. 2 are found by [34] as 193 N, 0.00148 s, and 0.0025 s respectively. Then coefficients a_0, a_n, and b_n for the Fourier series are determined from Eqs. (31-33), respectively as:

$$a_0 = 228.512\ sin(1.57079k) \tag{48}$$

$$a_n = \frac{30.7169 sin(1.57079k)}{n} sin(3.71965n) \tag{49}$$

$$b_n = \frac{30.7169 sin(1.57079k)}{n} [1 - cos(3.71965n)] \tag{50}$$

Coefficients a_0, a_n, and b_n for the first five harmonics are considered using Eqs. (49) and (50) to determine the forced response of the system. Considering up to fifth harmonics, the approximated force exerted by the water jet on the runner wheel for the one-sixteenth revolution of the runner is as shown in Fig. 4. The addition of higher-order harmonics increases ripples at the peak but does not affect the peak amplitude value significantly. Hence, harmonics up to the order of five are considered for further analysis.

4.3. Forced response of the system

Then using Eqs. (46 and 47), the steady-state response for the transverse vibration of the system considering up to the third mode is determined and presented in the graphical form. Substituting $x = L/4$, into the expressions obtained from Eqs. (46) and (47), the steady-state response for the transverse vibration of the shaft at its quarter length is obtained, and it can be presented in the form of response plots. as shown in Figs. 5 and 6.

Similarly, substituting $x = L/2$, into the expressions obtained from Eqs. (46) and (47), the steady-state response for the transverse vibration of the disk is obtained, and it can be presented in the form of response plots, as shown in Fig. 7 and Fig. 8.

From Figs. 5-8 it is found that the vibration amplitudes in the *y*-direction are significantly higher than that in the *z*-direction. A higher vibration amplitude in the *y*-direction is due to the impact of the jet. The vibration response in the *z*-direction is almost sinusoidal throughout the length of the shaft. The vibration response in the *y*-direction is almost sinusoidal in the region far from the disk, and it has a distorted form in the region near the midspan of the shaft or disk location.

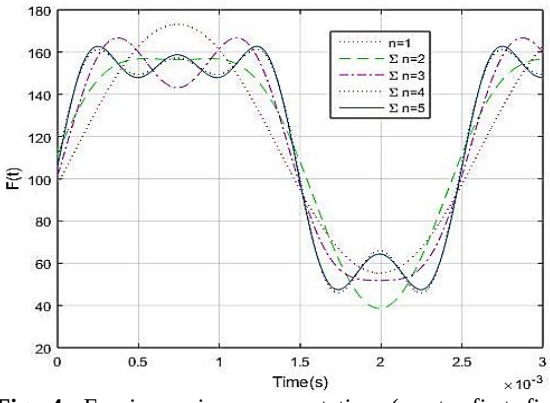

Fig. 4. Fourier series representation (up to first five harmonics n = 5) of the force exerted by the water jet.

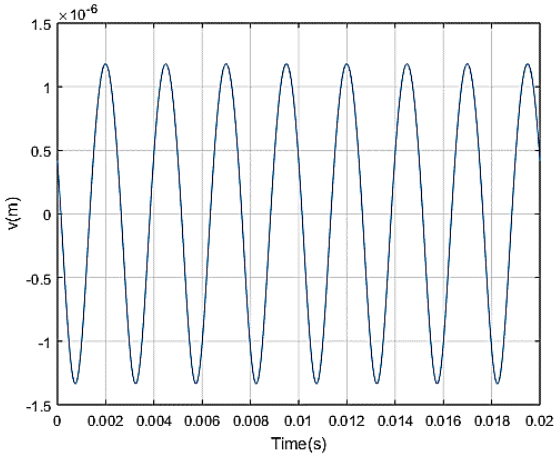

Fig. 5. Transverse displacement of shaft at $x = L/4$ in horizontal direction for Ω = 1500 rpm.

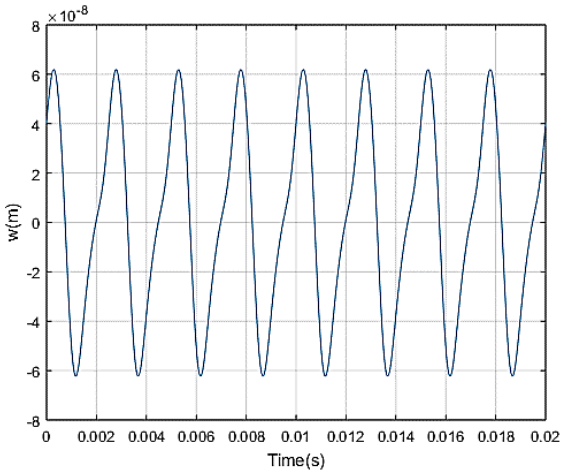

Fig. 6. Transverse displacement of shaft at $x = L/4$ in vertical direction for Ω = 1500 rpm.

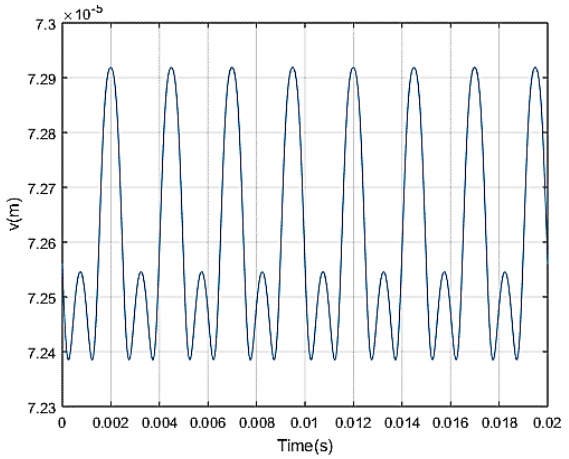

Fig. 7. Transverse displacement of disk in horizontal direction for Ω = 1500 rpm.

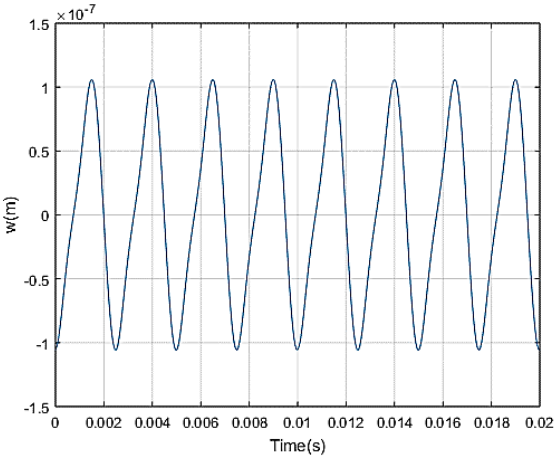

Fig. 8. Transverse displacement of disk in vertical direction for Ω = 1500 rpm.

5. Conclusions

In this paper, the dynamic behavior of the Pelton turbine is studied by modelling it as a rigid disk attached on an Euler-Bernoulli shaft. The governing equation of the system for bending vibrations in two transverse directions is found to be a coupled system of differential equations. Performing free vibration analysis, the critical speeds of the system for an operating speed of Ω = 1500 rpm for the first three modes are found to be 4001 rpm, 33644 rpm and 47944 rpm for the backward whirl and 7003 rpm, 38437 rpm and 50953 rpm for the forward whirl, respectively.

For the forced vibration analysis, the force provided by the water jet is approximated as the Fourier series up to the fifth harmonic components. Then, a steady-state response for bending vibration of the system is determined by applying the superposition principle. The peak amplitude of bending vibration at the midspan of the shaft (disk location) in the direction of the jet for an operating speed of Ω = 1500 rpm is found to be 73 μm. Similarly, the peak amplitude of bending vibration at the midspan of the shaft (disk location) in the vertical direction for an operating speed of Ω = 1500 rpm is found to be 0.1 μm.

Acknowledgement

The authors would like to acknowledge the partial support provided by the National Academy for Science and Technology, Nepal for this study.

References

[1] M. Sabuncu and A. Kacar, "Critical Speed M. Sabuncu and A. Kacar, "Critical Speeds of Continuous Shaft-Disc System, " *Vibration and Wear in High Speed Rotating Machinery*, pp. 241-251, (1990).

[2] C. Rajalingham, R. B. Bhat and G. D. Xistris, "Influence of External Damping on the Stability and Response of a Horizontal Rotor with Anisotropic Bending Stiffness," *Tribology Transactions*, pp. 393-398, (1993).

[3] C. W. Lee and J. S. Yun, "Dynamic Analysis of Flexible Rotors Subjected to Torque and Force," *Journal of Sound and Vibration* , Vol. 192, No. 2, pp. 439-452, (1996).

[4] N. Khader, A. Atoum and A. Al-Qaisia, "Theoretical and Experimental Modal Analysis of Multiple Flexible Disk-Flexible Shaft System," (2007).

[5] A. N. Silva and N.M.M. Maia, "Modelling a Rotating Shaft as an Elastically Restrained Bernoulli-Euler Beam," *Experimental Techniques*, Vol. 37, pp. 6-13, (2011).

[6] C. Chattoraj, S.N. Sengupta and M. C. Majumder, "Analysis of Dynamic Behaviour a Rotating Shaft with Central Mono-Disk," *International Journal of Engineering & Technology Research*, Vol. 2, No. 1, pp. 77-88, (2013).

[7] O. Gundogdu, K. Alnefaie and H. Diken, "Modelling and Analysis of a Jeffcott Rotor as a Continuous Cantilever Beam and an Unbalanced Disk System," *Gazi University Journal of Science Part A: Engineering And Innovation*, Vol. 2, No. 1, pp. 77-85, (2014).

[8] M. Shahgholi and S. E. Khadem, "Analysis of Stability and Bifurcation of an Asymmetrical Rotor," in *Proceedings of the ASME 2015 Dynamic Systems and Control Conference*, Columbus, Ohio, USA, (2015).

[9] X. Lin, R. Zhou and N. Xiao, "Influence Characteristics of Shaft and Disk Models on Natural Frequency of Single-Rotor System," *Applied Mechanics and Materials*, Vol. 607, pp. 490-494, (2014).

[10] D. J. Han, "Complex Harmonic Modal Analysis of Rotor Systems," *Journal of Mechanical Science and Technology*, Vol. 29, pp. 2735-2746, (2015).

[11] G. Huang, "Characteristics of Torsional Vibration of a Shaft with Unbalance," *Journal of Sound and Vibration*, Vol. 308, No. 3-5, pp. 692-698, (2007).

[12] C. O. Chang and J. W. Cheng, "Non-linear Dynamical and Instability of a Rotating Shaft-Disk System," *Journal of Sound and Vibration* , Vol. 160, No. 3, pp. 433-454, (1993).

[13] G. Genta and C. Delprete, "Acceleration Through Critical Speeds of an Anisotropic, Non-Linear Torsionally Stiff Rotor with Many Degrees of Freedom," *Journal of Sound and Vibration* , Vol. 180, No. 3, pp. 369-386, (1995).

[14] T. Inoue and Y. Ishida, "Chaotic Vibration and Internal Resonance Phenomena in Rotor Systems," *Journal of Vibration and Acoustics, Transactions of the ASME*, Vol. 128, No. 2, pp. 156-169, (2006).

[15] H. Diken and I. G. Tadjbakhsh, "Non-Linear Vibration Analysis and Subharmonic Whirl Frequencies of the Jeffcott Rotor Model," *Journal of Sound and Vibration*, Vol. 243, No. 1, pp. 117-125, (2001).

[16] R. Shad, G. Michon and A Berlioz, "Modelling and analysis of nonlinear rotordynamics due to higher order deformations in bending," *Applied Mathematical Modelling*, Vol. 35, No. 5, pp. 2145-2159, (2011).

[17] P. Phadatare and B. Pratiher, "Nonlinear Frequencies and Unbalanced Response Analysis of High Speed Rotor-Bearing Systems," *Procedia Engineering*, Vol. 144, pp. 801-809, (2016).

[18] O. Al-Bedoor, "Modelling the coupled torsional and lateral vibrations of unbalanced rotors," *Comput. Methods Appl. Mech. Engrg.*, Vol. 190, No. 45, pp. 5999-6008, (2001).

[19] L. Xiang and S. Yang, "Analysis of Flexural and Torsional Vibration for Turbogenerator Shafts on Power Impact," *Advanced Materials Research*, Vol. 139-141, pp. 2498-2501, (2010).

[20] K. Alnefaie, "Lateral and Longitudinal Vibration of a Rotating Flexible Beam Coupled with Torsional Vibration of a Flexible Shaft," *World Academy of Science, Engineering and Technology*, Vol. 7, No. 5, pp. 317-324, (2013).

[21] H. Kojima and K. Nagaya, "Nonlinear Torsional Vibrations of a Rotating Shaft System with a Magnet Couplling,"

Bulletin of the JSME, Vol. 27, No. 228, pp. 1258-1263, (1984).

[22] A. Muszynska and P. Goldman, "Chaotic Responses of Unbalanced Rotor/Bearing/Stator Systems with Looseness or Rubs," *Chaos, Solitons & Fractals*, Vol. 9, No. 9, pp. 1683-1704, (1995).

[23] M. Behzad and M. Asayesh, "Vibration Analysis of Rotating Shaft with Loose Disk," *IJE Transactions B: Applications*, Vol. 15, No. 4, pp. 385-393, (2002).

[24] A. Azeez and A. F. Vakakis, "Numerical and experimental analysis of a continuous overhung rotor undergoing vibro-impacts," *International Journal of Non-Linear Mechanics*, Vol. 34, No. 3, pp. 415-435, (1999).

[25] X. Shen, J. Jia and M. Zhao, "Numerical Analysis of a Rub-impact Rotor-bearing System with Mass Unbalance," *Journal of Vibration and Control*, Vol. 13, No. 2, pp. 1819-1834, (2007).

[26] C. Jian and C. K. Chen, "Chaos of rub–impact rotor supported by bearings with nonlinear suspension," *Tribology International*, Vol. 42, No. 3, pp. 426-439, (2009).

[27] Khanlo, M. Ghayour and S. Ziaei-Rad, "Chaotic vibration analysis of rotating, flexible, continuous shaft-disk system with a rub-impact between the disk and the stator," *Commun Nonlinear Sci Numer Simulat*, Vol. 16, No. 1, pp. 566-582, (2011).

[28] Khanlo, M. Ghayour and S. Ziaei-Rad, "The effects of lateral–torsional coupling on the nonlinear dynamic behaviour of a rotating continuous flexible shaft–disk system with rub–impact," *Commun Nonlinear Sci Numer Simulat*, Vol. 18, No. 6, pp. 1524-1538, (2013).

[29] W. Jiao, Q. Yuan and Y. Chang, "Study on the coupled bending-torsional vibration of unbalanced rotor system with external excitations," *IEEE International Conference on Computer Science and Automation Engineering (CSAE)*, (2012).

[30] H. Ma, X. Y. Tai, H. L. Yi, S. Lv and B. C. Wen, "Nonlinear dynamic characteristics of a flexible rotor system with local rub-impact," *Journal of Physics: Conference Series*, Vol. 448, (2013).

[31] X. Tai, H. Ma, F. Liu, Y. Liu and B. Wen, "Stability and steady-state response analysis of a single rub-impact rotor system," *Arch Appl Mech*, Vol. 85, pp. 133-148, (2013).

[32] A. M. Wahab, Z. A. Rasid and A. Abu, "Parametric Instability of Static Shafts-Disk System Using Finite Element Method," in *5th Asia Conference on Mechanical and Materials Engineering (ACMME 2017)*, Vol. 241, (2017).

[33] L. Chen, J. Wang, Q. Han and F. Chu, "Nonlinear dynamic modelling of a simple flexible rotor system subjected to time-variable base motions," *Journal of Sound and Vibration*, Vol. 404, pp. 58-83, (2017).

[34] S. Karki, M. C. Luintel and L. Poudel, "Dynamic Response of Pelton Turbine Unit for Forced Vibration," in *IOE Gradauate Conference*, Kathamndu, (2017).

How to cite this paper:

Mahesh Chandra Luintel and Tri Ratna Bajracharya, *"*Dynamic response of a Pelton turbine shaft under the impact of water jet*", Journal of Computational and Applied Research in Mechanical Engineering,* Vol. 10, No. 1, pp. 73-84, (2020).

DOI: 10.22061/jcarme.2019.4636.1562

URL: http://jcarme.sru.ac.ir/?_action=showPDF&article=1043